

© Copyright 1993 American Meteorological Society (AMS). Permission to use figures, tables, and brief excerpts from this work in scientific and educational works is hereby granted provided that the source is acknowledged. Any use of material in this work that is determined to be “fair use” under Section 107 of the U.S. Copyright Act or that satisfies the conditions specified in Section 108 of the U.S. Copyright Act (17 USC §108, as revised by P.L. 94-553) does not require the AMS’s permission. Republication, systematic reproduction, posting in electronic form on servers, or other uses of this material, except as exempted by the above statement, requires written permission or a license from the AMS. Additional details are provided in the AMS CopyrightPolicy, available on the AMS Web site located at (<http://www.ametsoc.org/AMS>) or from the AMS at 617-227-2425 or [copyright@ametsoc.org](mailto:copyright@ametsoc.org).

Permission to place a copy of this work on this server has been provided by the AMS. The AMS does not guarantee that the copy provided here is an accurate copy of the published work.

## IMPROVING AIRCRAFT IMPACT ASSESSMENT WITH THE INTEGRATED TERMINAL WEATHER SYSTEM MICROBURST DETECTION ALGORITHM

Michael P. Matthews and Timothy J. Dasey

Lincoln Laboratory  
Massachusetts Institute of Technology

### 1. INTRODUCTION

In recent years a number of aircraft accidents have resulted from a small scale, low altitude wind shear phenomena known as a microburst. Microbursts are produced within thunderstorms and are characterized by intense downdrafts which spread out after impacting the earth's surface, displaying strong divergent outflows of wind. They are often associated with heavy rainfall, but can occur without surface rainfall (Wolfson, 1988).

The Terminal Doppler Weather Radar (TDWR) program is the first system developed to detect microbursts from a ground-based radar in the airport terminal area. Improving safety is its primary goal, and test operations in Denver, Kansas City, and Orlando have shown it to be highly successful in identifying microbursts. In general, this identification has been performed with a > 90% Probability of Detection (POD) and a < 10% Probability of False Alarm (PFA) (Merritt et al., 1989).

The Integrated Terminal Weather System (ITWS) will introduce several new low-level wind shear products. These products include the Microburst Prediction product, the Microburst Trend product, and an improved Microburst Detection Product. The Microburst Prediction product will provide estimates of the future location, onset time, and peak intensity of microbursts before their surface effects are evident (Wolfson et al., 1993). The Microburst Trend product is responsible for warning users about expected increases, over a two minute interval, in wind shear intensity along the approach and departure corridors of a runway. This two minute time period approximates the delay between pilot receipt of an alert and the time of actual encounter with the event. The trend product should serve to improve pilot information when making decisions involving a wind shear event. This is particularly important for currently weak, but rapidly intensifying, wind shears.

The Improved Microburst Detection Algorithm being developed under the ITWS program attempts to build on the performance of the TDWR Microburst algorithm by improving POD and PFA and providing finer localization capabilities. More importantly, enhancements to the TDWR algorithm are necessary in order to

1. provide a consistent input to the microburst trend algorithm.

2. closely relate the microburst alert to the energy loss that the aircraft will actually experience and to alerts from an on-board forward-looking Doppler radar.

The TDWR algorithm does a good job detecting the microburst impacted airspace, but makes no attempt to deduce the number and centers of the events. Since the resultant alert shapes are uncorrelated over time, performing a more detailed meteorological analysis, such as location tracking, and size and intensity projections required by the microburst trend product, are compromised. This motivating factor for the improved Microburst Detection Algorithm is discussed in more detail in other works (Dasey, 1993a, Dasey, 1993b).

The focus of this paper is on the second motivating factor listed above: relating the microburst alert more closely with actual aircraft performance. Much of this understanding has evolved from the analysis of data from instrumented aircraft penetrations of microbursts within the Orlando terminal area, coincident with TDWR testbed operation (Matthews and Berke, 1993, Campbell et al., 1992). The microburst penetration flights were conducted by NASA Langley, the University of North Dakota (UND), and several manufacturers of forward-looking wind shear detection systems, including Bendix, Rockwell-Collins, and Westinghouse. Use of this data has allowed comparison of the alert representation from the TDWR Microburst algorithm with that of the initial ITWS algorithm in terms of its relationship with aircraft performance.

Section 2. describes a wind shear hazard index, called the F Factor, and its estimation from a ground-based Doppler radar. The estimated F Factors from the TDWR alert shapes are described in section 3. Direct use of TDWR base data for computing shear is explored in section 4, as is the correlation of that data with aircraft F Factor measurements. Estimation of the F Factor from alert shapes output from the initial ITWS detection algorithm is explored in section 5. Section 6 examines the results and emphasizes future research.

### 2. THE WIND SHEAR HAZARD INDEX

In recent years, the aviation research community has moved from the classification of microburst intensity in terms of headwind/tailwind loss, to the rate of change of aircraft energy loss. This is especially true in the development of the airborne windshear sensors which need to relate the instantaneous impact of a microburst on the aircraft. This numerical microburst hazard index, called the F Factor, is a dimensionless measure proposed by Roland Bowles (Bowles, 1990) of NASA Langley Research Center. The Total F Factor ( $F_t$ ) is composed of two terms, the horizontal term ( $F_h$ , effect of headwind/tailwind loss on aircraft performance), and the vertical term ( $F_v$ , effect of the downdraft on aircraft performance). On board the aircraft, a reactive system uses the wind measuring instrumentation to calculate the F Factor and issues an *in situ* alert if the F Factor rises above a defined threshold.

---

*Corresponding author address:* Michael P. Matthews, M.I.T. Lincoln Laboratory, 244 Wood St., Mail Stop HW29-136, Lexington, MA 02173, Ph. 617/981-7430, E-mail: mpm@ll.mit.edu. The work described here was sponsored by the Federal Aviation Administration. The United States Government assumes no liability for its content or use thereof.

The straightforward way to verify the accuracy of ground-based windshear measurements is to fly an instrumented aircraft into wind shear under the observation of a ground-based detection system, then compare the measured performance impact of the aircraft with that of the ground-based system. The deployment of a testbed TDWR system by MIT Lincoln Lab and the need to test predictive airborne systems by NASA Langley Research Center presented a unique opportunity to validate the ground-based system against the *in situ* aircraft measurements on a large scale. Initial testing involved comparing the peak F Factor experienced by the plane with that reported by the TDWR.

### 3. TDWR ESTIMATION OF F FACTOR

Estimation of F Factor can be done using a modified version of the F Factor equation (Bowles, 1990):

$$F_T = K' \frac{\Delta V}{\Delta R} \left( \frac{GS}{g} + \frac{2h}{TAS} \right) = F_h + F_v \quad (1)$$

where  $K'$  is a constant,  $\Delta V$  is the velocity difference,  $\Delta R$  is the distance over which the velocity difference is computed,  $GS$  is the groundspeed of the aircraft,  $TAS$  is the true air speed of the aircraft,  $g$  is the gravitational constant, and  $h$  is the height of the radar beam. Since the Doppler radar is only capable of measuring the wind component along a radial, the vertical component needs to be estimated using the Doppler data. This was done by using a simplified version of the mass continuity equation. To do this the outflow region is assumed to be a cylinder with the radar beam acting as the top of the cylinder and the ground acting as the bottom. Therefore, what flows into the top of the cylinder (downdraft), must flow out the sides of the cylinder as outflow. With this model, the outflow is directly proportional to the downdraft depending upon the radius of the cylinder and the deceleration profile with height.

The TDWR microburst algorithm defines a microburst outflow region by fitting a race track shaped icon around groups of radar radial velocity segments that show sufficient velocity differential along their length. Site adaptable parameters control the maximum size of a shape, the minimum shape radius, and other shape characteristics. Each icon is assigned a value denoting the peak-to-peak velocity difference contained within the shape. The peak-to-peak velocity difference of the icon represents the largest velocity difference for any velocity segment within the icon. This value is used as the  $\Delta V$  term of equation (1), while the length of the segment with the largest peak-to-peak loss is used as the  $\Delta R$ .

For each of the 118 microburst penetrations, an F factor was calculated from the output of the Lincoln version of the TDWR microburst algorithm using the techniques described above. Figure 1 is a plot of the TDWR estimated total F factor (TDWR  $F_T$ ), compared to the *in situ* F factor. From the figure it can be seen that the computed TDWR  $F_T$  was consistently higher than the *in situ* F factor. Most notable is that the estimation was biased especially high for the NASA events.

The unexpectedly high values of TDWR  $F_T$  may be due to several factors, the most obvious of which is that the F factor computed from the microburst alarms assumes that the shear has a constant value at all points within the alarm's boundary. This assumption is incorrect, and since the aircraft sampled only a small portion of the area enclosed by the microburst alarms, it is quite possible that on many occasions they missed the localized "hotspot" of shear that caused the large

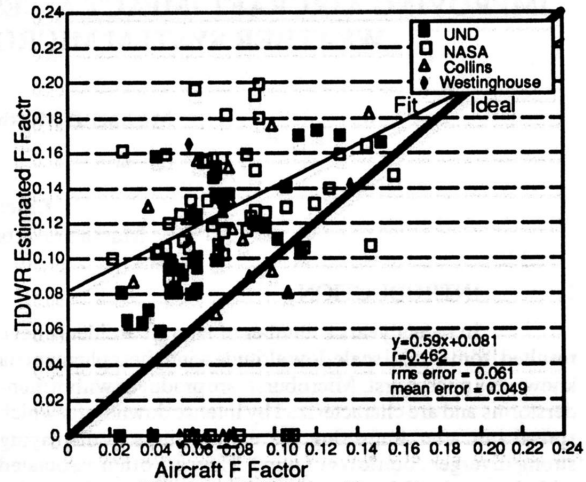


Figure 1. TDWR algorithm output vs. aircraft total F factor

value reported by the TDWR. The test pilots indicated during interviews that they occasionally avoided the most severe portion of a storm intentionally due to flight safety considerations. This limitation of the TDWR microburst algorithm, required the development of a method to calculate F Factor on an along track basis. Work in the airborne windshear community pointed to using radial shear to compute an F Factor.

### 4. TDWR SHEARMAP ESTIMATION OF F FACTOR

F factors can be computed from the TDWR testbed's radial velocity data by creating a map of the radial shear. To do this, the radar base data were first subjected to a data quality editing process and then velocity dealiasing. The data quality editing consisted of clutter removal, point-target editing, and range obscuration editing. Next, the velocity field was median filtered using a sliding window of approximately 500 meters x 500 meters. The actual radial shear computation for each range gate was calculated by performing a least squares fit on seven gates centered about the point. With the TDWR radar's 150 meter gate spacing, this resulted in a fit over a radial distance of 1050 meters. This general method of shear computation is similar to work done by Britt (Britt, 1992) for NASA's airborne Doppler windshear detection system.

The peak F factor can then be estimated along the trajectory of the aircraft by using the closest radial shear value as calculated from the TDWR base data. To do this analysis, the F Factor was broken down into its two terms, horizontal and vertical. From equation 1, the horizontal term can be calculated directly from the TDWR shear map data using the following formula (Note:  $K'$  is equal to one because the shear map is a one kilometer shear):

$$F_H = \frac{\Delta V}{\Delta R} \left( \frac{GS}{g} \right) \quad (2)$$

Figure 2 compares the horizontal term of the F factor as estimated from the TDWR shear map and the aircraft. The shear map provides a fairly good estimate of the horizontal F factor, but tends to overestimate. A possible explanation for an overestimated F factor from the shear map is the difference between the altitude of the aircraft and the radar beam. For most of the events, the aircraft penetrated the microburst at a much higher altitude than the radar beam. Physical observa-

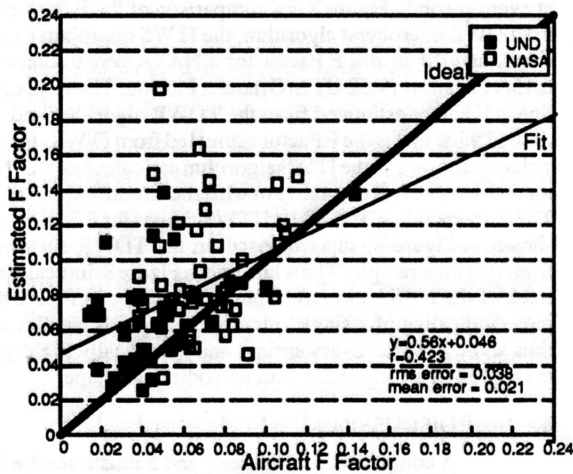


Figure 2. TDWR shearmap vs. aircraft horizontal F Factor at F total peak time

tions and modeling results suggest that the horizontal shear in a microburst typically decreases with altitude. Thus, it would seem prudent to attempt to compensate for the discrepancy between the height at which the TDWR antenna beam and the aircraft measured the microburst intensity.

The Oseguera and Bowles (Oseguera and Bowles, 1988) analytical microburst model includes a vertical shaping function for the horizontal wind velocity that is a good fit to experimental data. Correcting for altitude, Figure 3 shows that there is a marked improvement in the shear map estimates for horizontal F factor. Therefore, using the shear map and correcting for altitude seems to provide an acceptable estimation of the horizontal F factor.

From formula (1), the vertical term of the F factor is estimated using the following formula (Again: K' is equal to one because the shear map is a one kilometer shear):

$$F_v = \frac{\Delta V}{\Delta R} \left( \frac{2h}{TAS} \right) \quad (3)$$

Figure 4 shows the shear map estimated vertical term versus the *in situ* F factor. The vertical estimation perfor-

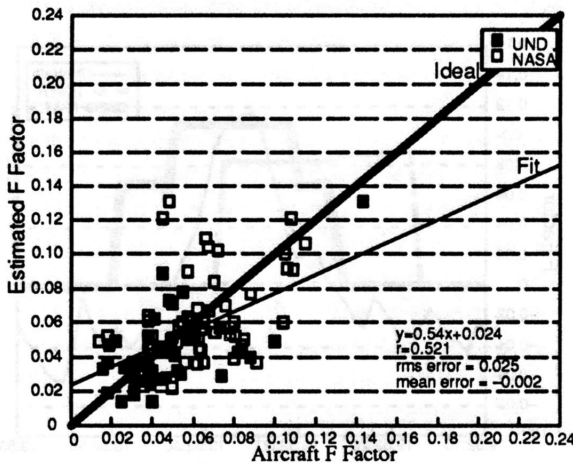


Figure 3. TDWR shearmap vs. aircraft horizontal F Factor at F total peak time using altitude profile correction

mance is sufficient when penetrating the center of a weak to moderate microburst. However, when the aircraft penetrated the edge of a microburst there was some overestimation, and when the aircraft encountered a strong microburst, there was some underestimation.

While the current TDWR microburst algorithm performs extremely well in detecting microburst hazards, some enhancements are needed to improve its ability to characterize the impact the windshear will have on aircraft performance. Research has shown that the current TDWR microburst shapes overestimate the hazard if the aircraft does not encounter the core of the microburst. A shear-based approach was developed that, after altitude compensation, provided an acceptable means to estimate the F Factor. This research, along with research in the airborne community, has demonstrated that using radial shear as a means to characterize the impact a microburst will have on an aircraft is more accurate than methods currently used.

## 5. ITWS ESTIMATION OF F FACTOR

The ITWS microburst detection algorithm uses the shearmap data from the TDWR base data, as discussed in the previous section, as its primary data source. It operates by locating segments of radial shear with an average shear above defined threshold levels (Dasey, 1992a). Currently, the algorithm thresholds at 4 shear intervals (4.0, 6.0, 8.0, and 10.0 m/s/km). These segments are constrained to avoid containing too many bad data points or negative shear values. Then for each threshold level, segments on adjacent radials are associated with one another into regions of shear. For each region a loss value is determined from the radial velocity by taking a velocity difference between two points for which the average shear is above 2.5 m/s/km. Next, a circular shape is optimized to best fit the resulting regions, and is tested for sufficient peak shear and loss for a wind shear alert (minimum 15 knots, 5.0 m/s/km) or a microburst alert (minimum 30 knots, 10.0 m/s/km).

One of the goals of the ITWS microburst detection algorithm is to more accurately characterize the strength, in terms of F Factor, of a microburst. Estimation of F Factor can be done for the ITWS algorithm by using the horizontal equation of the F Factor (Equation 2.) and substituting the  $\Delta V/\Delta R$  term with the shear value of the microburst as detected by ITWS. Before doing this an altitude compensation can be applied to the data, similar to that done when computing F Factor

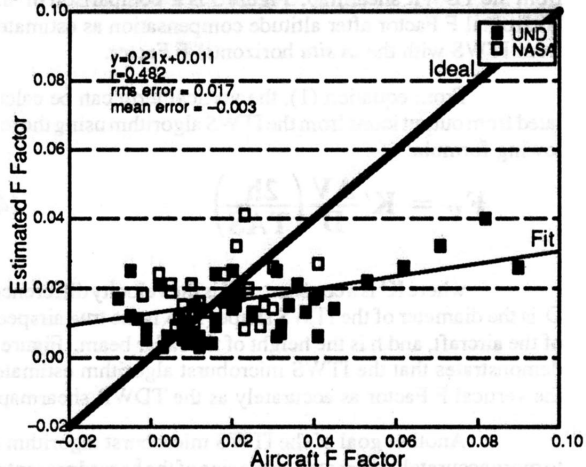


Figure 4. TDWR shearmap vs. aircraft vertical F Factor at F total peak time



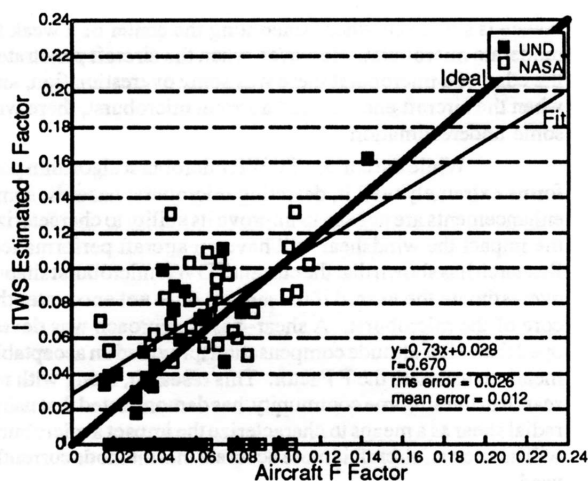


Figure 5. ITWS algorithm output vs. aircraft horizontal F Factor at Ftotal peak time

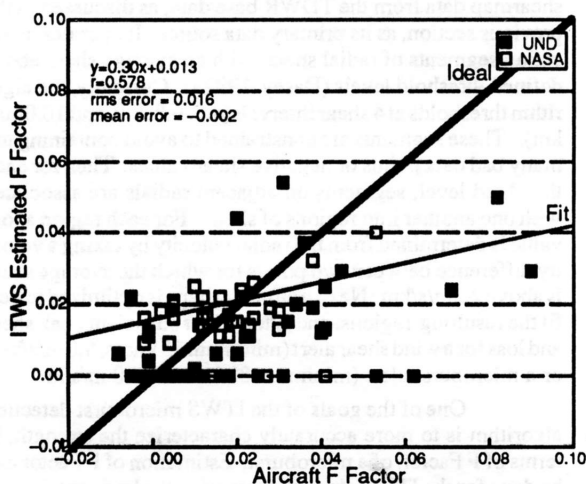


Figure 6. ITWS algorithm output vs. aircraft vertical F Factor at Ftotal peak time

from the TDWR shearmap. Figure 5 is a comparison of the horizontal F Factor after altitude compensation as estimated from ITWS with the *in situ* horizontal F Factor.

From equation (1), the vertical term can be calculated from output icons from the ITWS algorithm using the following formula:

$$F_v = K' \frac{\Delta V}{D} \left( \frac{2h}{TAS} \right) \quad (4)$$

where  $K'$  is a constant,  $\Delta V$  is the velocity difference,  $D$  is the diameter of the ITWS shape,  $TAS$  is the true airspeed of the aircraft, and  $h$  is the height of the radar beam. Figure 6 demonstrates that the ITWS microburst algorithm estimates the vertical F Factor as accurately as the TDWR shearmap.

Another goal of the ITWS microburst algorithm is to more accurately characterize the size of the hazard presented to an aircraft from windshear. To do this the along-track trajectory total F Factor can be compared to the estimated F Factor

at every second. Figure 7 is a comparison of the F Factor for the TDWR microburst algorithm, the ITWS microburst algorithm, and the *in situ* F Factor for a NASA penetration of a 6/15/91 event at 19:52 UT in Orlando, Florida. The solid thick line is F Factor estimated from the TDWR algorithm and the dashed thick line is the F Factor estimated from ITWS. Figure 7 clearly shows that the ITWS algorithm can calculate an F factor which is more representative of what the aircraft experiences. The corresponding TDWR and ITWS shapes for this event are shown in Figure 8, superimposed on the TDWR shearmap from that time sample. The white line in Figure 8 indicates the track of the NASA aircraft. The ITWS shape in Figure 8 is more indicative of a single microburst event, is smaller and thus should reduce overwarning, and specifically highlights the region of strong shear with an additional shape.

## 6. DISCUSSION

A comparison of Figures 1 and 5 illustrates the improved F Factor representation the ITWS detection algorithm gives over the TDWR microburst detection algorithm. More impressively, the ITWS performance in Figure 5 is comparable to the results from the TDWR shearmap in Figure 3.

Of the events in Figure 5 with no ITWS detection (ITWS shear output was zero), there are two possible explanations for these failures. First, some of the events penetrated by the aircraft where in their development stages. Since the Doppler data are only capable of measuring the horizontal flow, any event in its development stage (i.e. downdraft) will go undetected. A solution to this problem is to incorporate the ITWS microburst prediction product, which provides information about the location and intensity of downdrafts, in addition to other aloft information. In other cases, the aircraft flew along a track which fell just outside an ITWS icon. The ITWS program is being tuned with this and other information to put out icons of a size that will reduce these misses.

Several improvements are expected to be made in both the F factor estimation algorithm and the ITWS detection algorithm. First, a function which corrects vertical F factor estimates for the distance from the center of the microburst will be added. This is particularly crucial for the ITWS algorithm, which has the philosophy of alerting with one icon per event. Secondly, on going data analysis efforts are underway to determine the accuracy and overall performance of the ITWS microburst detections. As more results become available,

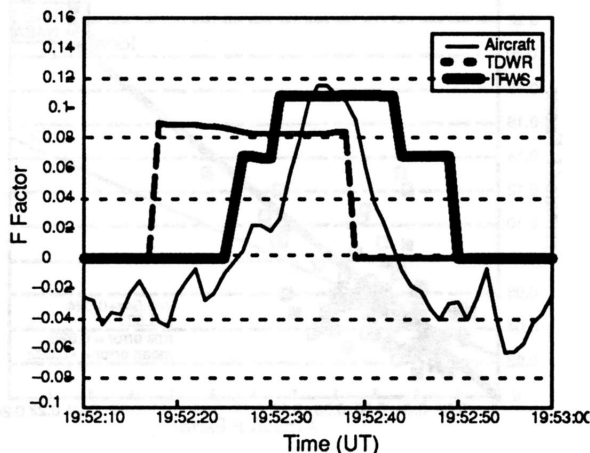


Figure 7. F Factor estimated from TDWR and ITWS for NASA case on 6/15/91 in Orlando.

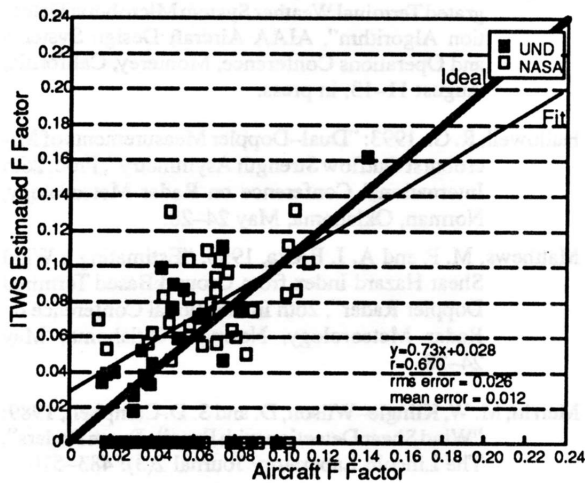


Figure 5. ITWS algorithm output vs. aircraft horizontal F Factor at Ftotal peak time

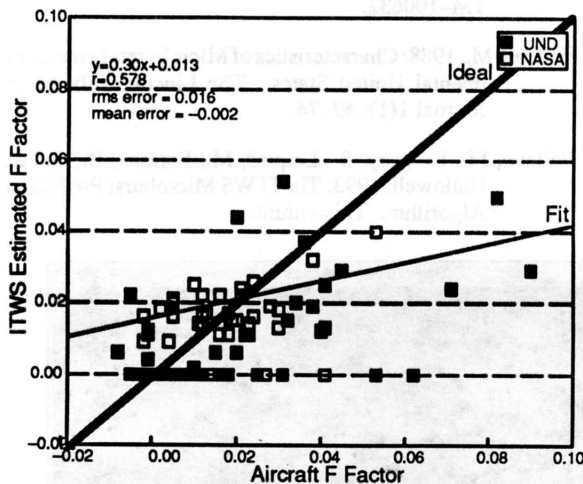


Figure 6. ITWS algorithm output vs. aircraft vertical F Factor at Ftotal peak time

from the TDWR shearmap. Figure 5 is a comparison of the horizontal F Factor after altitude compensation as estimated from ITWS with the *in situ* horizontal F Factor.

From equation (1), the vertical term can be calculated from output icons from the ITWS algorithm using the following formula:

$$F_v = K' \frac{\Delta V}{D} \left( \frac{2h}{TAS} \right) \quad (4)$$

where  $K'$  is a constant,  $\Delta V$  is the velocity difference,  $D$  is the diameter of the ITWS shape,  $TAS$  is the true airspeed of the aircraft, and  $h$  is the height of the radar beam. Figure 6 demonstrates that the ITWS microburst algorithm estimates the vertical F Factor as accurately as the TDWR shearmap.

Another goal of the ITWS microburst algorithm is to more accurately characterize the size of the hazard presented to an aircraft from windshear. To do this the along-track trajectory total F Factor can be compared to the estimated F Factor

at every second. Figure 7 is a comparison of the F Factor for the TDWR microburst algorithm, the ITWS microburst algorithm, and the *in situ* F Factor for a NASA penetration of a 6/15/91 event at 19:52 UT in Orlando, Florida. The solid thick line is F Factor estimated from the TDWR algorithm and the dashed thick line is the F Factor estimated from ITWS. Figure 7 clearly shows that the ITWS algorithm can calculate an F factor which is more representative of what the aircraft experiences. The corresponding TDWR and ITWS shapes for this event are shown in Figure 8, superimposed on the TDWR shearmap from that time sample. The white line in Figure 8 indicates the track of the NASA aircraft. The ITWS shape in Figure 8 is more indicative of a single microburst event, is smaller and thus should reduce overwarning, and specifically highlights the region of strong shear with an additional shape.

## 6. DISCUSSION

A comparison of Figures 1 and 5 illustrates the improved F Factor representation the ITWS detection algorithm gives over the TDWR microburst detection algorithm. More impressively, the ITWS performance in Figure 5 is comparable to the results from the TDWR shearmap in Figure 3.

Of the events in Figure 5 with no ITWS detection (ITWS shear output was zero), there are two possible explanations for these failures. First, some of the events penetrated by the aircraft where in their development stages. Since the Doppler data are only capable of measuring the horizontal flow, any event in its development stage (i.e. downdraft) will go undetected. A solution to this problem is to incorporate the ITWS microburst prediction product, which provides information about the location and intensity of downdrafts, in addition to other aloft information. In other cases, the aircraft flew along a track which fell just outside an ITWS icon. The ITWS program is being tuned with this and other information to put out icons of a size that will reduce these misses.

Several improvements are expected to be made in both the F factor estimation algorithm and the ITWS detection algorithm. First, a function which corrects vertical F factor estimates for the distance from the center of the microburst will be added. This is particularly crucial for the ITWS algorithm, which has the philosophy of alerting with one icon per event. Secondly, on going data analysis efforts are underway to determine the accuracy and overall performance of the ITWS microburst detections. As more results become available,

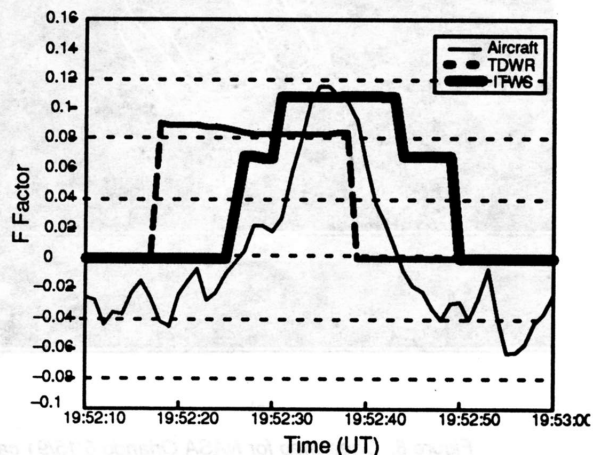


Figure 7. F Factor estimated from TDWR and ITWS for NASA case on 6/15/91 in Orlando.

changes will be made in the methods to further refine the ITWS microburst algorithm. Also, future work on the ITWS algorithm is planned to incorporate data from the Low Level Wind Shear Alert System (LLWAS). This should improve ability to detect asymmetric microbursts by providing data which is perpendicular to the radar beam (Hallowell, 1993), and ensure a consistent wind shear alert from systems within the terminal area.

## REFERENCE

- Bowles, R. L., 1990: "Reducing Windshear Risk Through Airborne Systems Technology", 17th Congress on the Aeronautical Sciences, Stockholm, Sweden, Sep. 9-14.
- Britt, C. L., and Bracalante, E., 1992: "NASA Airborne Radar Windshear Detection Hazard Algorithm and the Detection of Wet Microbursts in the Vicinity of Orlando Florida," Airborne Wind Shear Detection and Warning Systems, Fourth Combined Manufacturers' and Technologists' Conference, Williamsburg, Virginia, (April 1992).
- Campbell, S. D., Berke, A. J. and M. P. Matthews, 1992: Orlando TDWR Testbed Results. Proc. Fourth Combined Manufacturers and Technologists' Airborne Wind Shear Review Meeting.
- Dasey, T. J., 1993: "A Shear Based Microburst Detection Algorithm for the Integrated Terminal Weather System (ITWS)", 26th International Conference on Radar Meteorology, Norman, Oklahoma, May 24-28.
- Dasey, T. J., 1993: "The Design and Motivation for the Integrated Terminal Weather System Microburst Detection Algorithm", AIAA Aircraft Design Systems and Operations Conference, Monterey, California, August 11-13, in press.
- Hallowell, R. G., 1993: "Dual-Doppler Measurements of Microburst Outflow Strength Asymmetry", Proc. 26th International Conference on Radar Meteorology, Norman, Oklahoma, May 24-28.
- Matthews, M. P. and A. J. Berke, 1993: "Estimating a Wind Shear Hazard Index from Ground Based Terminal Doppler Radar", 26th International Conference on Radar Meteorology, Norman, Oklahoma, May 24-28.
- Merritt, M. W, Klinge-Wilson, D. and S. D. Campbell, 1989: "Wind Shear Detection with Pencil-Beam Radars", The Lincoln Laboratory Journal 2(3): 483-510.
- Oseguera, R. M. and R. L. Bowles, 1988: "A Simple Analytic 3-Dimensional Downburst Model Based on Boundary Layer Stagnation Flow", NASA TM-100632.
- Wolfson, M., 1988: Characteristics of Microbursts in the Continental United States. The Lincoln Laboratory Journal 1(1): 49-74.
- Wolfson, M., Delanoy, R., Leipins, M., Forman, B., and R. Hallowell, 1993: The ITWS Microburst Prediction Algorithm. This volume.



Figure 8. Shearmap for NASA Orlando 6/15/91 case overlaid with (a) TDWR microburst shapes, (b) ITWS shapes.